

Colloidal QDs-polymer nanocomposites

H. Gordillo, I. Suárez, P. Rodríguez-Cantó, R. Abargues, R. García-Calzada, V. Chyrvony, S. Albert, and J. Martínez-Pastor

UMDO (Unidad Asociada al CSIC-IMM), Instituto de Ciencia de los Materiales, Universidad de Valencia, PO Box 22085, 46071 Valencia, Spain
Henry.gordillo@uv.es

ABSTRACT

Nanometer-size colloidal semiconductor nanocrystals, or Quantum Dots (NQD), are very prospective active centers because their light emission is highly efficient and temperature-independent. Nanocomposites based on the incorporation of QDs inside a polymer matrix are very promising materials for application in future photonic devices because they combine the properties of QDs with the technological feasibility of polymers. In the present work some basic applications of these new materials have been studied. Firstly, the fabrication of planar and linear waveguides based on the incorporation of CdS, CdSe and CdTe in PMMA and SU-8 are demonstrated. As a result, photoluminescence (PL) of the QDs are coupled to a waveguide mode, being it able to obtain multicolor waveguiding. Secondly, nanocomposite films have been evaluated as photon energy down-shifting converters to improve the efficiency of solar cells.

Keywords: **colloidal QD, nanocomposite, PMMA, SU8, waveguides, solar cells.**

1. INTRODUCTION

Nowadays photonic research is going towards the design of novel functional materials able to perform more complex and efficient tasks. For this purpose, nanocrystals or colloidal quantum dots (NQDs) are very promising candidates to be incorporated as active medium in new optoelectronic devices. The reason of this choice comes from the feasibility provided by colloidal chemistry [1] allowing the tuning of the absorption and emission wavelength by the control of the nanoparticle radius (1nm to 10nm) during the synthesis process [2]. As a consequence of their small size, NQDs show strong quantum confinement, being its emission practically temperature independent [3]. Moreover, chemical methods allow to control the emission wavelength changing not only the NQDs size but also their base material without modifying their surface chemistry. In this way the NQDs emission can cover a broad range of the optical spectrum using CdS [4], CdTe [5] and CdSe [6] in the visible range, and PbS [7], PbSe and InAs [8] in the near infrared.

In order to incorporate these nanoparticles into functional devices NQDs have to be dispersed in a solid state matrix [9]. Such a multicomponent material is called nanocomposite, and have the advantages of joining the quantum confinement provided by the NQD with the technological feasibility of the matrix. For this purpose polymers are very attractive as materials to hold the nanoparticles for several reasons. They are cheap, flexible, easily processed into films by coating techniques and patternable by UV lithography or e-beam [10]. It has already been demonstrated the use polymers as a matrix for metal nanoparticles [11] and organic dyes [12], resulting in a broad range of applications like optical amplification [13], photovoltaics [14], sensing [15] and plasmonics [16]. Moreover, the fact that most polymers are highly transparent at wavelengths longer than 400 nm makes them a suitable material for waveguiding. Then, nanocomposites based on the dispersion of NQD in polymers are very promising active material to be used in integrated optical devices.

In this way NQDs-polymer nanocomposites have been already fabricated, to implement a microcavity laser [17] or to obtain two color waveguiding by means of the incorporation of two families of QDs (CdSe and CdTe) into a PMMA matrix [18] (see figure 1 left). As well NQD-polymer nanocomposites can be good materials for photon energy down-shifting conversion in silicon solar cells [19, 20]. In these applications QDs with strong absorption in the UV region and high photoluminescence (PL) in the visible region are selected in order to shift the incident light wavelengths from UV, where the spectral response of the solar cell is low, to the ones where the silicon solar cell is sensitive (visible region). In

this way the efficiency of the solar cell can be markedly improved without modification of its design, by placing the nanocomposite on the cell. A schematic figure of an example of a spectral down-converter is shown in figure 1 right.

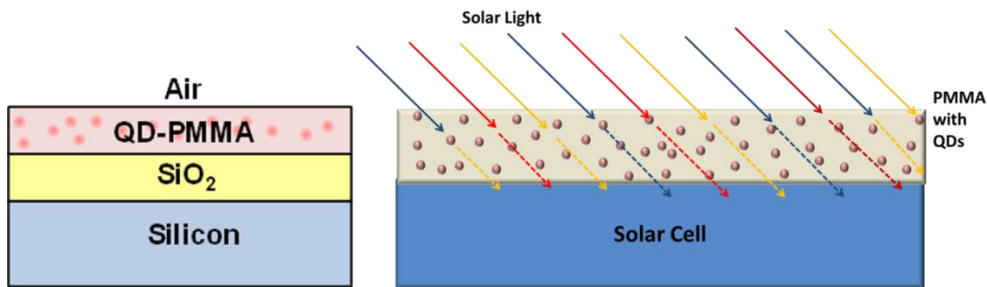


Figure 1. Left QDs-PMMA waveguide structure. Right, QDs-nanocomposite applied on top of a solar cell.

In this work the fabrication of nanocomposites based on the dispersion of NQDs in a PMMA matrix is proposed for waveguiding and photovoltaic applications. This polymer is cheap, optically transparent above 400 nm and can be deposited by solution-processed techniques. Then, NQD-PMMA nanocomposites can act as a core of planar waveguides when they are deposited on a substrate with lower refractive index (SiO_2/Si). As a result, using appropriate concentrations, PL of QDs can be coupled to the waveguide modes, doing it possible to obtain multicolor waveguiding when more than one emitting nanostructure is dispersed in the matrix. As an example CdS (450 nm), CdTe (550 nm) and CdSe (600 nm) are embedded in PMMA demonstrating the simultaneous waveguiding of blue, green and orange colors in the same structure. Then, these results are extrapolated to a polymer with photolithographic properties (SU8) in order to implement ridge photoluminescent patterns. Finally, a thoroughly study of the absorption of CdSe-PMMA and CdS-PMMA nanocomposites deposited on a glass substrate is presented, in order to obtain the optimum conditions for down-shift light converters.

2. EXPERIMENTAL PROCEDURE

2.1 NQDs-PMMA nanocomposites

Nanocomposites have been prepared by mixing two solutions containing NQDs and the PMMA. In order to allow a good dispersion in the matrix, toluene has been chosen as a common solvent of the different sorts of QDs (CdS, CdTe and CdSe), which have been used in this work, being in all cases synthesized by the process developed by Peng's group [21]. Once the solution is prepared, it is deposited on the substrate (glass or SiO_2) by spin coating. The resulting film was exposed to two baking processes at temperatures of 80°C and 150 °C during 2 minutes each during two minutes. The concentration of QDs into the PMMA depends on the application needed. For example, for waveguiding the concentration has to be adjusted to obtain an optimal filling factor between 10^{-3} and 10^{-4} according to the results obtained elsewhere [18]. Nevertheless, for solar cells applications the absorption QDs is the most important target and a higher quantity of nanoparticles is used.

The different NQDs (CdS, CdSe, CdTe) used here have different optical transitions due to their differences in chemical nature and sizes. Figure 2 shows the absorbance and PL spectra of the three QD colloids. The exciton peaks in the absorption spectra of CdS, CdTe and CdSe QDs are placed at 436nm, 537nm and 580nm, respectively. For shorter wavelengths the absorbance increases continuously and excited states are observed. This exciton transition corresponds to QD radius of 2.5 nm for CdSe, 4.5 nm for CdS and 1.5 nm for CdTe, approximately, according to literature results [22]. The PL spectra of colloidal NQDs (dashed lines) present a Stokes shift of 40 nm (the shift between the PL and the exciton ground state absorption peak) [23]. PL peaks of CdS, CdSe and CdTe are centered at 454 nm, 560 nm and 620nm, their FWHM (Full Width at Half Maximum) being of 20 nm, 30 nm and 40 nm, respectively. The broad band centered at 600 nm for CdS NQDs is related to emission associated to surface states [24]. The PL spectra of NQDs-PMMA nanocomposites are shown as continuous red lines. The Stokes-shift is now smaller than in colloidal state for

CdTe and CdSe nanocomposites (PL peak centered at 546nm and 609nm, respectively), because the NQDs tend to agglomerate in a more important proportion [25].

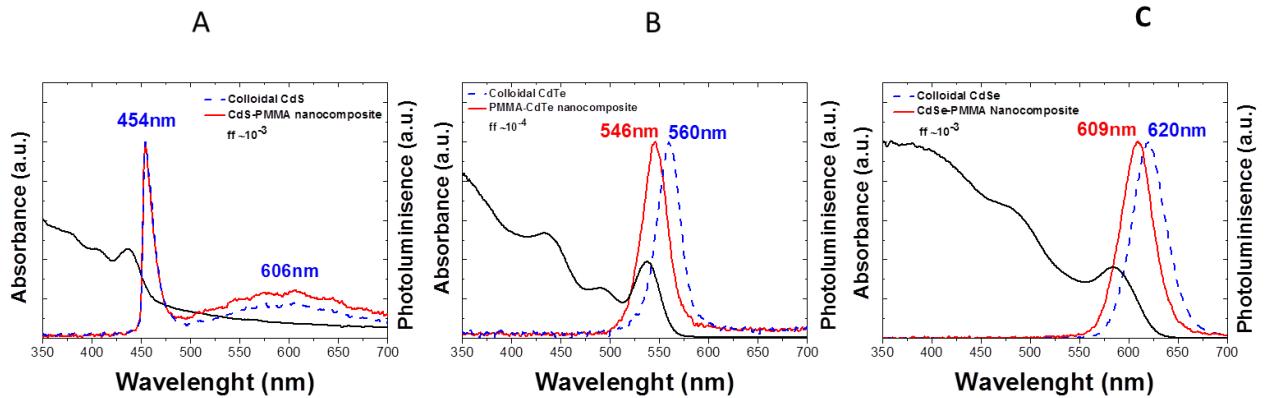


Figure 2. The absorptions and PL spectra of colloidal solutions and nanocomposite thin films of CdS (A), CdTe (B) and CdSe (C) QDs. The black lines correspond to the colloidal QDs absorbance spectra, the red lines to the PL from the nanocomposites and the dash blue lines correspond to the colloidal QDs PL.

2.2 Sample preparation and experimental set-up

For fabricating planar waveguides the nanocomposite solution is deposited on a SiO_2/Si substrate. The thickness of the films was in the range 1-2 μm , as shown in Fig. 3-left. In these conditions, the NQD-PMMA film (refractive index $n \sim 1.489$ at 600nm) acts as an active core of the structure, and the SiO_2 acts as low refractive index cladding layer ($n \sim 1.458$ at 600nm). Ridge waveguides were elaborated by patterning SU-8 ($n \sim 1.511$ at 600 nm) straight lines on the SiO_2 -Si substrate following the procedure recommended by the manufacturer [26]. The polymer was spin coated on the substrate, and exposed to two bakes at 65°C and 95°C. Then, the film was exposed to UV radiation during 3 seconds and post baked again at 65 °C and 95 °C. The time of baking was 2 minutes in all cases. At the end of the process, 4, 6, 8, 10 and 20 μm wide and 2 μm high ridge waveguides were defined on the substrate, as illustrated in Fig. 3-right. The waveguiding properties of the structures were characterized by end-fire coupling a laser beam at the input edge of the sample using a microscope objective, and collecting the output light with another microscope objective. Also, samples were illuminated from its top surface using a cylindrical lens to focus the excitation. The excitation light source chosen in both configurations was a 404 nm GaN diode laser in order to use a source able to pump the nanostructures. PL spectra were obtained focusing the collected light to an optical fiber connected to a spectrograph (StellarNet EPP2000). In Fig. 4 the experimental set-up is shown. The blue box shows a picture of the light coupling system. PL measurements of the nanocomposites and colloidal solutions were made by collecting the back-scattered light from the dropped solution on a glass substrate, and using the same laser source (GaN 404 nm) and collecting system (optical fiber + spectrograph).

The samples prepared to study the transmission of NQD-PMMA nanocomposite for solar cells applications consisted of CdSe- PMMA and CdS-PMMA thin films deposited by spin coating on a transparent glass substrates, and baked in the way mentioned before. In order to obtain the optimum conditions for downshift converters, samples with different filling factors and thicknesses have been studied. Optical transmission spectra of the nanocomposite layers were measured by using a commercial reflectometer (Nanocalc-2000 from Mikropack).

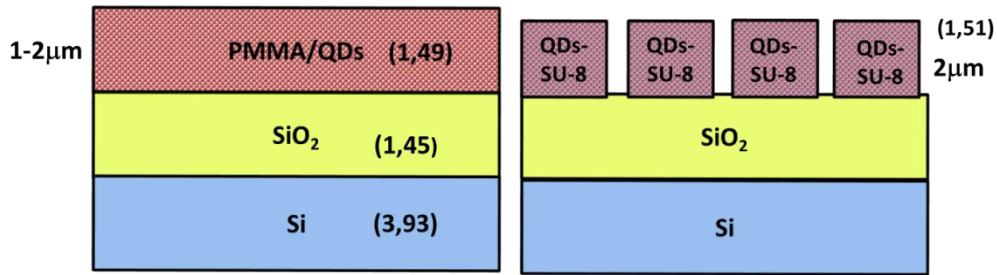


Figure 3. Structure of the waveguides. Left: planar QD-PMMA waveguide, Right: QD-SU8 ridge waveguides.

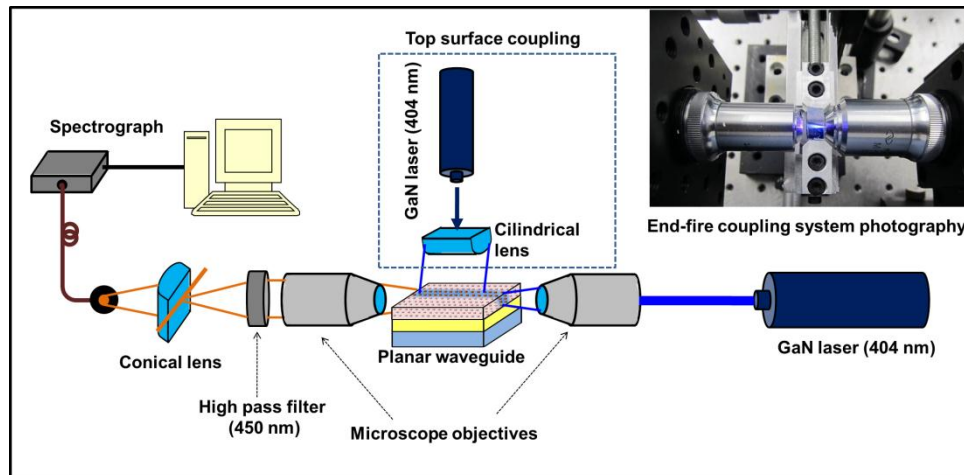


Figure 4. Experimental set-up for characterizing the NQD based waveguides. The inset shows a picture of the end-fire coupling system.

3. QD-PMMA NANOCOMPOSITE WAVEGUIDES

Planar nanocomposite waveguides have been characterized using the experimental set-up shown in Fig. 4. It has been already demonstrated [18] that for low enough filling factors ($ff \sim 10^{-3}$ or less) NQD-PMMA waveguides demonstrate small propagation losses, doing it possible to end-fire-couple the 404 nm GaN pumping laser and to see waveguided PL at the output of the structure. For higher filling factors ($\sim 10^{-3}$) the PL can not be guided by this coupling system due to absorption losses of the nanostructure [perdidas por scattering ??? en este caso mayor quitar y dejar solo absorption losses]. Waveguided PL can be also obtained by focusing the laser beam in the form of a straight line on the top surface of the sample. When yet higher QD concentrations are dispersed in the nanocomposite it was not possible to obtain any waveguiding due to the high level absorption losses.

A typical PL spectrum measured in a planar CdSe-PMMA waveguide is shown in Fig. 5, where optical pumping was performed from the top surface of the sample. The PL guided spectrum has a maximum at 613 nm and a FWHM of 42 nm. The inset of the figure shows that the PL intensity has a linear dependence with the pumping power, hence because not all QDs states are filled at the maximum available pumping power [18].

When the concentration of NQDs is decreased, the waveguided PL emission of a nanocomposite film is broader and shifts to shorter wavelengths. This effect is shown in Fig. 6, where guided PL spectra are presented using the filling factor as a parameter. The PL peak goes from 580 nm for a filling factor of 1.8×10^{-4} to 613 nm for a filling factor of 4.4×10^{-3} . This observation can be likely accounted for by the PL reabsorption effect, which is much higher from the short wavelength side of the PL spectrum, where absorption and PL spectra overlap. At lower filling factors the contribution of the reabsorption decreases, which is accompanied by the short wavelength shift of the PL spectrum.

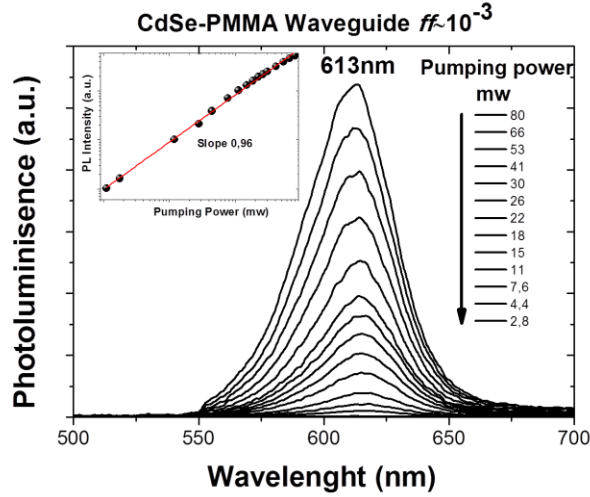


Figure 5. Waveguiding PL spectra from a planar CdSe-PMMA waveguide obtained by the top surface coupling as a function of the pumping power. On the inset, the PL integrated intensity dependence with the pumping power is depicted.

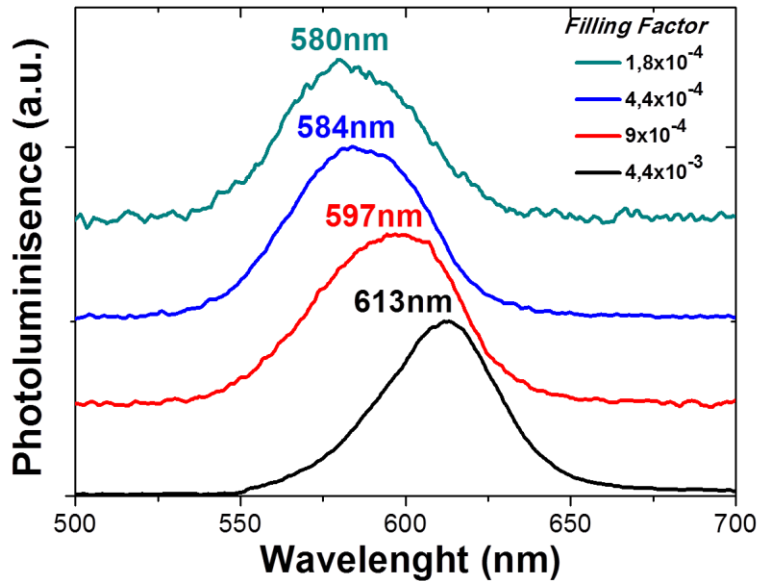


Figure 6. PL guided emission spectra for several filling factors of NQDs in the nanocomposite. The measurements were made with top surface optical coupling.

3.1 Multicolor waveguiding

The results obtained for waveguiding using CdSe-PMMA films can be extrapolated to other kinds of quantum dots. Moreover, it is possible to disperse in the same photonic structure different NQDs in order to demonstrate multicolor waveguiding. Three different colors using CdSe, CdTe and CdS is proposed here to show the use of these nanocomposites in white emission applications [28] [29]. For this purpose, the concentration of the QDs families has to be chosen carefully in order to avoid reabsorption between the different NQDs families [18]. The measured PL spectrum in the NQD-PMMA waveguide is shown in Fig. 7 (hollow circles) that exhibits three peaks centered at 452 nm, 551 nm and 590 nm. This PL spectrum can be nicely fitted by using three Gaussian contributions (continuous red line)

corresponding to the three ensembles of NQDs (CdS, CdTe and CdSe). In top panel of Fig. 7 the pictures of the three waveguided colors are shown: blue for CdS, green for CdTe and orange for CdSe ensembles.

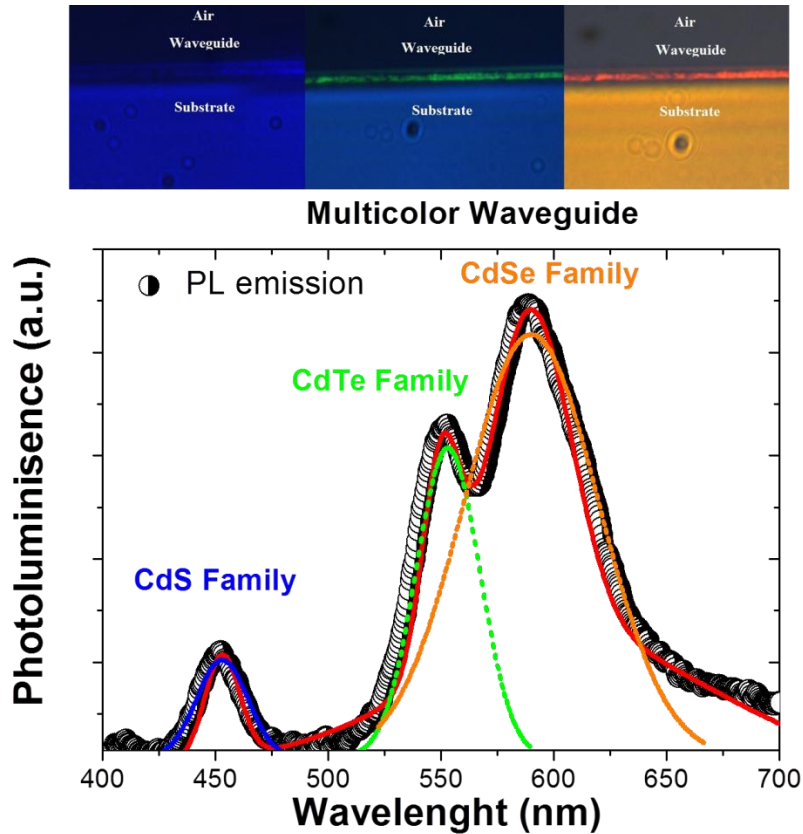


Figure 7. Waveguiding PL spectrum in a PMMA waveguide doped with CdS, CdTe and CdSe NQDs. The pictures at the top panel correspond to guided colors: CdS (left), CdTe (middle) and CdSe (right).

3.2 CdSe-SU8 ridge waveguides

One of the most useful characteristics of polymers resides on the possibility to be patterned, that is necessary in the fabrication of photonic microstructures for integrated optical devices. In this way SU8 is one of the most interesting polymers due to its high refractive index, robust characteristics and easy patterning. In this way a new nanocomposite based on the dispersion of NQDs in SU8 is proposed [27]. For this purpose the correct ligand exchange on oleate-terminated QDs have been carried out in order to make the nanoparticles soluble in a solvent compatible with SU8 (for example γ -butyrolactone) [27]. The fabrication of ridge waveguides made with the NQD-SU8 nanocomposite was successful: waveguided PL mode distributions for different waveguide widths is demonstrated (top panel of Fig. 8). The measured PL spectrum in one of these ridge waveguides is centered at 610 nm (Fig. 8).

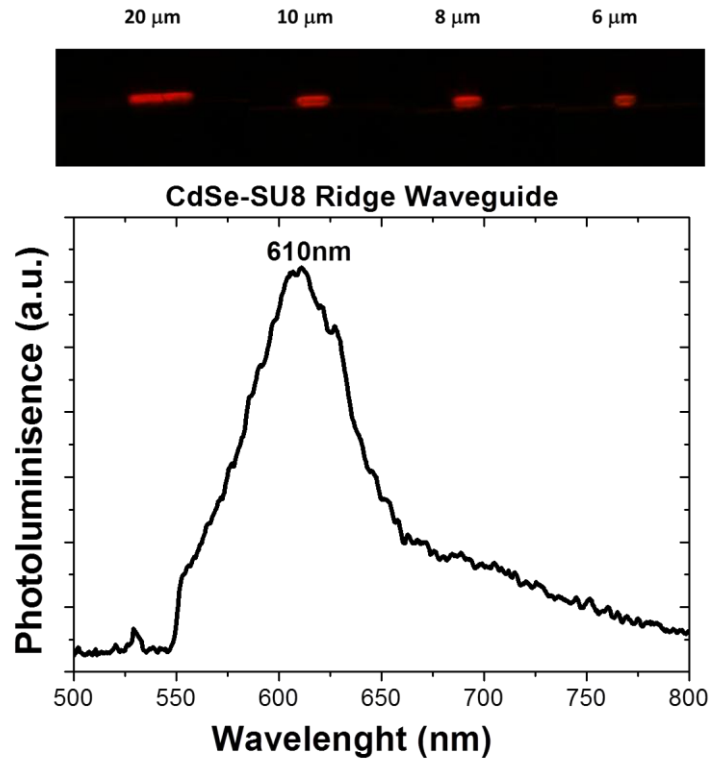


Figure 8. Waveguiding PL spectrum of a CdSe-SU8 ridge waveguide. The picture at the top panel shows the guided PL at ridge waveguides of different widths.

4. QD-PMMA NANOCOMPOSITES FOR SOLAR CELLS

NQD-PMMA nanocomposites are useful not only for photonic applications but also for solar cells. Due to their high absorption in the UV and their PL in the visible (see Fig. 2), CdS-, CdTe- or CdSe-PMMA films could be used to convert UV radiation to the visible region in order to improve the efficiency of solar cells. For this purpose the film should possess a high absorption in the UV (near 90 %) with good transmittance in the visible (around 90 %). In order to explore the feasibility of NQD-PMMA for this application, the absorbance spectrum is studied as a function of the volume fraction of NQDs at the nanocomposite, or filling factor (ff), and the layer thickness. Firstly, CdSe NQD-PMMA films 1.5 μm thick were prepared by depositing the nanocomposites on glass, and varying the concentration of NQDs in the film. The absorbance spectra of the CdSe-PMMA layers as a function of the ff are shown in Fig. 9, where a maximum absorbance around 40% is reached for the highest ff . However, the increase of the NQD concentration in the film is accompanied by a simultaneous increase of the absorbance for wavelength longer than that of the absorption edge ($\lambda_0 \approx 600\text{nm}$). This undesirable effect for the downshift converter should be attributed to scattering of light, because the NQDs does not exhibit appreciable absorption for $\lambda > \lambda_0$ (Fig. 2C). It is more important for higher ff because of NQD aggregation is more probable producing an increase of the concentration of light scatters inside the nanocomposite and film surface roughness. Therefore, an intermediate filling factor has to be chosen in order to obtain a reasonable compromise between absorption at the UV and light scattering at the transparent wavelengths ($\lambda > \lambda_0$). Figure 10 shows the absorbance spectra of a CdS NQD-PMMA nanocomposite for $ff \approx 10^{-2}$ and the thickness of the layer as a parameter. It is worth to say that CdS NQDs seems to be more suitable than CdSe NQDs for solar cells applications, because its gap is closer to the UV region leaving a larger transparent window in the visible region. The absorbance clearly increases with the thickness being it possible to obtain 70 % of absorption at 300 nm with a nanocomposite film thickness $\approx 17.5 \mu\text{m}$. However, as long as the thickness is increased the transmittance of the film again decreases down to 80 % in the

region where the film should be transparent. Therefore, there is a contradiction between good absorption in the UV region and the light scattering losses in the visible ($\lambda > \lambda_0$) that could limit the application of NQD-nanocomposites to be useful for light downshift conversion. In this case, light scattering is limited by surface roughness of the thin film because of our deposition method: a stack of spin coated nanocomposite layers. This limitation can be overcome by fabricating the film with use of Doctor Blade instrument instead of spin coating. This method allows the deposition of thicker layers with good homogeneity and low roughness. Figure 11 shows the absorbance a 0.5 mm thick layer of CdS-PMMA deposited with use of Doctor Blade instrument on a glass substrate and exposed to two bakes at 80 °C and 150 °C during 2 minutes each. For wavelengths below 350 nm absorption is higher than 75 %, while it is lower than 5% for wavelengths longer than the absorption edge ($\lambda_0 \approx 450$ nm).

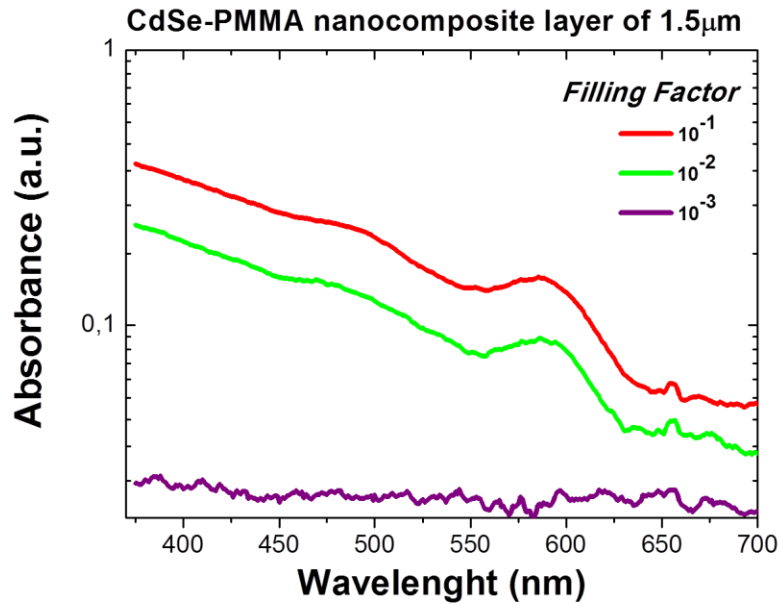


Figure 9. Absorbance spectra (in logarithmic scale) of CdSe-PMMA nanocomposite as a function of the NQD filling factor.

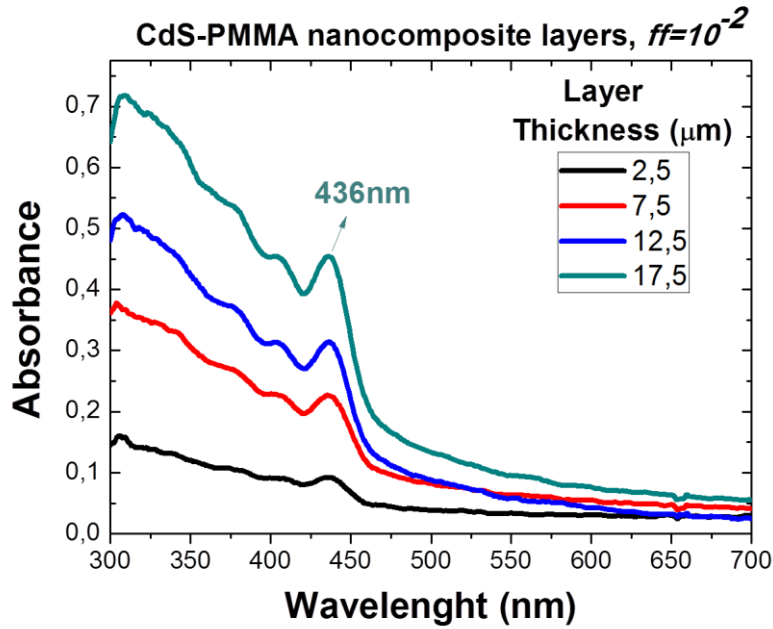


Figure 10. Absorbance spectra of CdS-PMMA nanocomposite thin films as a function of the layer thickness for $ff \sim 10^{-2}$.

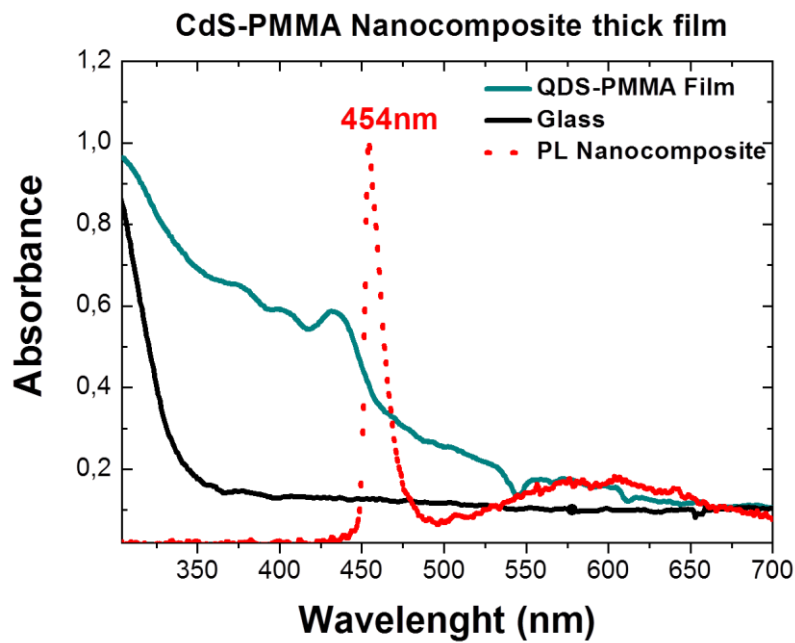


Figure 11. Absorbance spectra of CdS-PMMA nanocomposite thick film. The blue line correspond to nanocomposite film and the black one to the glass substrate. The red line correspond to the PL emission of the nanocomposite.

5. CONCLUSIONS

In this work the integration of nanocrystal QDs into a polymer matrix to form nanocomposite films useful for integrated photonic devices and solar cells is explored, being two very prospective lines of application demonstrated. First, thin

films fabricated by the dispersion of colloidal quantum dots (CdS, CdSe and CdTe) in polymer can act as optical planar waveguides when they are embedded in a PMMA layer. As a result, their photoluminescence can be coupled to the waveguide modes, doing it possible to obtain multicolor waveguiding when more than one QD family is dispersed in the matrix. As a second step, CdSe is dispersed in SU8 in order to fabricate ridge waveguides able to confine PL in two dimensions. Finally, the use of the nanocomposites for spectral down-conversion of the incident light in solar cell is studied, the results obtained indicate that thick (~0.5 mm) QD-PMMA layers with lower QD filling factors give better results as compared to thin (a few μm) layers possessing much higher filling factors because lower QD concentration allows to avoid QD aggregation, which is responsible for parasitic light scattering over all the incident light spectrum.

ACKNOWLEDGMENTS

This work has been supported by the EU FP7 under the project NanoPV (NMP-246331), by the "Ministerio de Educación" under the project TEC-2011-29120-C05-01, and by the "Generalitat Valenciana" through the PROMETEO 2009/074 grant and GRISOLIA program (Henry Gordillo).

REFERENCES

- [1] Alivisatos P., "Perspectives on the physical chemistry of semiconductor nanocrystals," *Journal of Physical Chemistry*, vol. 100, no. 31, 13226-13239 (1996).
- [2] Klimov V. I., "Nanocrystal quantum dots: from fundamental photophysics to multicolor lasing," *Los Alamos Science*, no. 28, 214-220 (2003).
- [3] Klimov V I, Mikhailovsky A A, Xu S, Malko A, Hollingsworth J A, Leatherdale C A, Eisler H J and Bawendi M G. "Optical Gain and Stimulated Emission in Nanocrystal Quantum Dots" *Science* no. 290, 314-317 (2000).
- [4] Chan Y., Stecke J. S. I., Snee P. T., Caruge J. M., Hodgkiss J. M., Nocera D. G. And Bawendi M. G., "Blue semiconductor nanocrystal laser," *Applied Physics Letters*, vol. 86, no. 7, pp. 073102 (2005).
- [5] D. Lourençoni Ferreira, F. Oliveira Silva, L. Cristina de Souza Viol, P. Licinio, M. Valadares, L. Alberto Cury, M. Antonio Schiavon and J. Luiz Aarestrup Alves, "Growth kinetics of CdTe colloidal nanocrystals," *Journal of Chemical Physics*, vol. 131, no. 8, 084712 (2009).
- [6] Chen Y., Herrnsdorf J., Guilhaert B., Zhang Y., Watson I. M., Gu E., Laurand N. And Watson M. D., "Colloidal quantum dot random laser," *Optics Express*, vol. 19, no. 4, 2996-3003 (2011).
- [7] Sukhovatkin V., Musikhin S., Gorelikov I., Cauchi S., Bakueva L., Kumacheva E. and E. Sargent H., "Room-temperature amplified spontaneous emission at 1300 nm in solution-processed PbS quantum-dot films," *Optics Letters*, vol. 30, no. 2, 171-173 (2005).
- [8] Wu Z., Mi Z., Bhattacharya P., Zhu T. And Xu J., "Enhanced spontaneous emission at 1.55 μm from colloidal PbSe quantum dots in a Si photonic crystal microcavity," *Applied Physics Letters*, vol. 90, no 171105 (2007).
- [9] Jasieniak J., Pacifico J., Signorini R., Chiasera A., Ferrari M., Martucci A. and Mulvaney P., "Luminescence and amplified stimulated emission in CdSe-ZnS-nanocrystal-doped TiO₂ and ZrO₂ waveguides," *Advanced Functional Materials*, vol. 17, no. 10, 1654-1662 (2007).
- [10] Uddin M. A. and Chan H. P., "Materials and process optimization in the reliable fabrication of polymer photonic devices," *Journal of Optoelectronics and Advanced Materials*, vol. 10, no. 1, 1-17 (2008).
- [11] Abargues R., Abderrafi K., Pedrueza E., Grades R. s, Marqués-Hueso J., Valdés J. L. and Martínez-Pastor J., "Optical properties of different polymer thin films containing in situ synthesized Ag and Au nanoparticles," *New Journal of Chemistry*, vol. 33, no. 8, 1720-1726 (2009).
- [12] Reilly M. A., Marinelli C., Morgan C. N., Penty R. V., White I. H., Ramon M., Ariu M. and D. Bradley D. C., "Rib waveguide dye-doped polymer amplifier with up to 26 dB optical gain at 625 nm," *Applied Physics Letters*, vol. 85, no. 22, 5137-5139 (2004).
- [13] Amarasinghe D., Ruseckas A., Turnbull G. A. and I. Samuel D. W., "Organic semiconductor optical amplifiers," *Proceedings of the IEEE*, vol. 97, no 9, 1637-1650 (2009).
- [14] Kramer I. J. and Sargent H., "Colloidal quantum dot photovoltaics: a path forward," *ACS Nano*, in press.
- [15] Gradess R, Abargues R, Habbou A, Canet-Ferrer J, Pedrueza E, Russell A, Valdes J L, Martinez-Pastor J P "Localized surface plasmon resonance sensor based on Ag-PVA nanocomposite thin films" *Journal of Materials Chemistry* 19, 9233-9240 (2009).

- [16] De Leon I. and Berini P., "Amplification of long-range surface plasmons by a dipolar gain medium," *Nature Photonics*, vol. 4, no. 6, 382-387, (2010).
- [17] Smirnova T. N., Sakhno O. V., Yezhov P. V., L. M. Goldenberg and Stumpe J., "Amplified spontaneous emission in polymer-CdSe/ZnS-nanocrystal-DFB structures produced by the holography method," *Nanotechnology*, vol. 20, no. 44, pp. 245707 (2009).
- [18] Suárez I., Gordillo H., Abargues R., Albert S. and Martínez-Pastor J., "Photoluminescence waveguiding in CdSe and CdTe QDs-PMMA nanocomposite films," *Nanotechnology*, vol. 22, no. 43, 435202 (2011).
- [19] Van stark W.G.J.H.M., Meijerik A., Schropp R.E.I., Van Roosmalen J.A.M., Lysen E.H., "Enhancing solar cells efficiency by using spectral converters", *Solar energy & Solar cells*, 87, 395-409 (2005).
- [20] Klampaftis E., Ross D., McIntosh K.R., Richards B.S., "Enhancing the performance of solar cells via luminescent down-shifting of the incident spectrum: A review", *Solar energy & Solar cells*, 93, 1182-1194 (2009).
- [21] Yu W. W. and Peng X., "Formation of high-quality CdS and other II-VI semiconductor nanocrystals in noncoordinating solvents: Tunable reactivity of monomers," *Angewandte Chemie-International Edition*, vol. 46, 15, 2559-2559 (2002).
- [22] Yu W. W., Qu L., Guo W. and Peng X., "Experimental determination of the extinction coefficient of CdTe, CdSe and CdS nanocrystals," *Chemistry of Materials*, vol. 15, no. 14, 2854-2860 (2003).
- [23] Demchenko A.P., "Advanced fluorescence reporters in chemistry and biology III: applications in sensing and imaging," Springer, Berlin, vol. 10 (2011).
- [24] Tang J., Brzozowski L., D. Barkhouse A. R., Wang X., Debnath R., Wolowiec R., Palmiano E., Levina L., A. Pattantyus-Abraham G., Jamakosmanovic D. and E. Sargent H., "Quantum dot photovoltaics in the extreme quantum confinement regime: the surface-chemical origins of exceptional air- and light-stability," *ACS Nano*, vol. 4, no.2, pp. 869-878 (2010).
- [25] Sharma H., Sharma S. N., Singh G. and Shivaprasad S. M., "Effect of ratios of Cd:Se in CdSe nanoparticles on optical edge shifts and photoluminescence properties," *Physica E*, vol. 31, no. 2, 180-186 (2006).
- [26] http://www.microchem.com/Prod-SU8_KMPR.html
- [27] to be published
- [28] Sapra S., Sergiy M., Klart A., Rogach A.L. and Feldman J., "Bright white-light emission from semiconductor nanocrystals: by chance and by design", *Advanced Materials*, 19, 569-572 (2007).
- [29] Doty C.E., Bennett C.J.C., Sabau A.S., Jellison G.E.Jr., Boudreaux P.R., Walker S.C. and Ott R., "Advanced method for increasing the efficiency of white light quantum dot leds", *Phys. Status Solidi A.*, 208, 8, 1980-1982 (2011).